ORIGINAL ARTICLE
https://doi.org/10.5653/cerm.2020.04105
pISSN 2233-8233 · eISSN 2233-8241
Clin Exp Reprod Med 2021;48(3):211-220

Protective effects of curcumin against methotrexate-induced testicular damage in rats by suppression of the p38-MAPK and nuclear factor-kappa B pathways

Leyla Kilinc[1,2], **Yesim Hulya Uz**[1]

[1]Department of Histology and Embryology, Faculty of Medicine, Trakya University, Edirne; [2]Department of Histology and Embryology, Faculty of Medicine, Akdeniz University, Antalya, Turkey

Objective: The present study aimed to investigate the possibility that curcumin (CMN) protects against methotrexate (MTX)-induced testicular damage by affecting the phospho-p38 (p-p38) mitogen-activated protein kinase (MAPK) and nuclear factor-kappa B (NF-κB) signaling pathways.
Methods: Eighteen male Wistar albino rats were randomly divided into three groups. The control group was given an intragastric administration of dimethyl sulfoxide (DMSO) daily for 14 days, the MTX group was given a single intraperitoneal dose of MTX (20 mg/kg) on the 11th day, and the MTX+CMN group was given intragastric CMN (100 mg/kg/day, dissolved in DMSO) for 14 days and a single intraperitoneal dose of MTX (20 mg/kg) on the 11th day. At the end of the experiment, all animals were sacrificed and the testicular tissues were removed for morphometry, histology, and immunohistochemistry. Body and testicular weights were measured.
Results: Body weights, seminiferous tubule diameter, and germinal epithelium height significantly decreased in the MTX group compared to the control group. Whereas, the number of histologically damaged seminiferous tubules and interstitial space width significantly increased in the MTX group. In addition, the number of p-p38 MAPK immunopositive cells and the immunoreactivity of NF-κB also increased in the MTX group compared to the control group. CMN improved loss of body weight, morphometric values, and histological damage due to MTX. CMN also reduced the number of p-p38 MAPK immunopositive cells and the NF-κB immunoreactivity.
Conclusion: CMN may reduce MTX-induced testicular damage by suppressing the p38 MAPK and NF-κB signaling pathways.

Keywords: Curcumin; Methotrexate; Nuclear factor-kappa; p38; Testis

Introduction

Methotrexate (MTX) is a folic acid antagonist used as a medication for the treatment of acute lymphoblastic leukemia; osteosarcoma; choriocarcinoma; lymphoma; breast, bladder, and head and neck cancers, as well as for the treatment of non-malignant diseases such as psoriasis and rheumatoid arthritis [1-3]. It is also effective for the termination of pregnancy [3]. Anticancer drugs such as MTX have lethal effects on cancer cells, but they also affect normal tissues that have a high proliferation rate, such as bone marrow, intestinal mucosa, and gonads [4]. In addition to its gonadotoxicity, MTX also has known mutagenic and teratogenic properties [5]. Therefore, the current recommendation is to cease MTX treatment in both female and male patients at least 3 months before a planned pregnancy [3]. A single dose of MTX administered to rats causes an increase in oxidative stress in the testes, thereby leading to infertility directly or

Received: September 22, 2020 · Revised: January 13, 2021 · Accepted: February 22, 2021
Corresponding author: **Yesim Hulya UZ**
Department of Histology and Embryology, Faculty of Medicine, Trakya University, Edirne 22030, Turkey
Tel: +90-235-7641-1403 Fax: +90-284-235-7652 E-mail: uzyhulya@gmail.com

*This study was supported by Trakya University Scientific Research Projects (TUBAP 2013/126).

through the toxic effects of MTX [6-8]. It has been reported that male individuals exposed to MTX exhibit oligozoospermia and structural chromosomal rearrangements [9].

Various signals related to cell proliferation, cell differentiation, and cell death are regulated by mitogen-activated protein kinases (MAPKs) [10]. In particular, p38 MAPK can be activated by a variety of cellular stresses, including oxidative stress, and is related to inflammation and programmed cell death (apoptosis) [10-13]. A cell culture study using the human bronchial cell line BEAS-2B confirmed that MTX increased p38 MAPK expression and dose-dependently increased p38 MAPK phosphorylation, whereas pre-treatment with the p38 MAPK inhibitor SB203580 decreased both p38 MAPK expression and phosphorylation [14]. An organ culture study using human nasal polyp cells showed that MTX caused apoptosis by increasing the levels of the phosphorylated forms of p38 MAPK in a dose-dependent manner [15]. These studies indicate a potential association between the p38 MAPK signaling pathway and MTX.

Another known effect of MTX is its ability to promote significantly increased activation and translocation of nuclear factor-kappa B (NF-κB) [16-19]. NF-κB is a protein complex containing specific transcription factors with known involvement in inflammatory and innate immune responses [20]. These responses are also considered to involve oxygen free radicals, so various antioxidant substances have been explored as agents for the prevention of the testicular damage caused by MTX [6-8,21-27].

An antioxidant compound that is receiving particular attention is curcumin (CMN), which has substantial anti-inflammatory, immunomodulatory, antitumoral, antipsoriatic, and wound-healing properties in addition to its antioxidant activity [28-35]. CMN is a delicious yellow-orange-colored spice with a wide range of pharmacological and biological activities. It is obtained from the rhizomes of a Curcuma longa, a plant belonging to the Zingiberaceae family [36,37]. CMN is widely used in Far Eastern and Asian countries, especially in India and China, in the food industry (as a sweetener, preservative, coloring, spice, etc.) and in traditional medicine as a treatment for inflammation, sprains, and other conditions [38-41]. Song et al. [42] reported that CMN could inactivate p38 MAPK and NF-κB in a rat enteritis model and that it improved the intestinal mucosal barrier. Similarly, CMN also showed a protective effect against testicular damage caused by cisplatin by blocking p38 MAPK and NF-κB expression [43]. The present study aimed to analyze the possible protective effect of CMN against MTX-induced testicular damage through a histological and immunohistochemical examination of phospho-p38 (p-p38) MAPK and NF-κB signaling pathways.

Methods

1. Animals

For this study, 18 male Wistar albino rats weighing between 250 and 300 g (age, 3 months) were obtained from the Trakya University Experimental Animals Research Unit. During the study period, all rats were kept at a temperature of 22°C ± 1°C with a 12-hour light/dark cycle. The animals were fed a standard pellet feed and had free access to tap water. The experimental part of the study was carried out with approval from the Animal Experiments Local Ethics Committee of Trakya University (No. TUHDYEK-2013/50).

2. Experimental design

The rats were randomly divided into three groups of six animals each (n = 6) to form the control, MTX, and MTX+CMN groups. CMN (Sigma-Aldrich, St. Louis, MO, USA) was prepared by dissolving in dimethyl sulfoxide (DMSO; Merck, Darmstadt, Germany). The control group was given an intragastric dose of DMSO (1 mL/kg) daily for 14 days. The MTX group was given a single intraperitoneal dose of MTX (20 mg/kg, Kocak Farma, 50 mg/5 mL, Tekirdag, Turkey) on the 11th day of the experiment. The MTX+CMN group was given intragastric CMN (100 mg/kg/day) daily for 14 days and a single intraperitoneal dose of MTX (20 mg/kg) on the 11th day of the experiment. The doses of CMN and MTX used in this study were determined as described in previous studies [28,44].

Twenty-four hours after the last dose of CMN, all animals were sacrificed under anesthesia with xylazine (Basilazin; Bavet, Bosensell, Germany) and ketamine (Ketasol; Richter Pharma, Wels, Austria), and the testes were rapidly excised. Routine procedures were used for histological and immunohistochemical examinations of the testicular tissue. The body weight of all animals was measured at the beginning and end of the experiment, and the weight of the testes was measured at the end of the experiment. The testes weight index (TWI) was calculated for each animal by taking into account the body weight and the sum of the weights of the right and left testes of the same animal, using the following formula: TWI: ([sum of the weights of right+left testes]/body weight) × 100.

3. Histological examinations

All testis tissues for histological and immunohistochemical evaluations were fixed in 10% neutral-buffered formalin (Sigma-Aldrich), dehydrated in an increasing ethanol series, and embedded in paraffin. Then, 5-μm-thick sections were cut from the paraffin-embedded testis tissues with a microtome (RM-2245; Leica, Wetzlar, Germany). The sections were deparaffinized in toluene, rehydrated through a series of decreasing ethanol concentrations, and stained with hematoxylin and eosin (H&E). After staining, the slides were dehydrated through a se-

https://doi.org/10.5653/cerm.2020.04105

ries of increasing ethanol concentrations, immersed in toluene, and covered with Entellan (Merck). The slides were then examined and photographed under a light microscope (Olympus BX51, Tokyo, Japan) equipped with a DP 20 digital camera attachment.

The seminiferous tubule diameter, the germinal epithelium height, and interstitial space width in H&E stained testes sections were measured with a light microscope at ×100 or ×400 magnification using an Imaging Analysis System ver. 2.11.5.1 (Kameram-Argenit, Istanbul, Turkey). These measurements were performed by evaluating the transverse sections of a total of 30 tubules in five fields. Thirty tubules were chosen as round or near-round in three testes sections of each animal [25].

Germinal series cell changes were assessed histologically by light microscopy examination of six testis sections of each animal at ×100 magnification according to the following criteria: detachment (detachment of cohorts of spermatocytes from the seminiferous epithelium), sloughing (release of clusters of germ cells into the lumen of the seminiferous tubule), and vacuolization (appearance of empty spaces in the seminiferous tubule). For each parameter, the average percentages of normal and damaged tubules were determined. Average percentages for each sample were obtained by dividing the number of histologically damaged (detachment, sloughing, and vacuolization) or normal round tubules by the total number of round tubules in the same field, and multiplying the result by 100. Three areas were evaluated for each section and their averages were analyzed [45].

4. Immunohistochemical Examination

For the immunohistochemistry procedure, testis sections were incubated overnight at 56°C and then deparaffinized in toluene. The sections were rehydrated in a decreasing ethanol series and then boiled in a microwave for 15 minutes in 10 mM citrate buffer (pH 6) for antigen retrieval. The sections were cooled for 20 minutes at room temperature and then incubated with hydrogen peroxide solution (Thermo Scientific/Lab Vision, Fremont, CA, USA) for 10 minutes to inhibit endogenous peroxidase activity. The sections were then washed with phosphate-buffered saline (PBS; Sigma-Aldrich), and blocking solution (Ultra V Block-Thermo Scientific/Lab Vision) was applied for 5 minutes in a humidified chamber to prevent nonspecific binding. The sections were then incubated overnight at 4°C with p-p38 MAPK antibody (monoclonal rabbit, 1:50 dilution; Cell Signaling Technology, Beverly, MA, USA) or for 1 hour at room temperature with NF-κB/p65 antibody (polyclonal rabbit, 1:100 dilution; Thermo Scientific/Lab Vision). The negative control consisted of PBS that replaced the primary antibody. The sections were washed with PBS, and biotinylated secondary antibody (Biotinylated Goat Anti-Polyvalent, Thermo Scientific/Lab Vision) was applied at room temperature for 10 minutes. After washing again with PBS, streptavidin-peroxidase (Thermo Scientific/Lab Vision) was applied for 10 minutes. After PBS washing, 3-amino-9-ethyl carbazole (AEC; Thermo Scientific/Lab Vision) was added as the chromogen. The sections were washed with distilled water for 5 minutes and then counterstained with hematoxylin. The sections were washed once again with tap water and then covered with an aqueous mounting medium (Vision Mount, Thermo Scientific/Lab Vision) [43,46].

The p-p38 MAPK immunopositive staining index was determined at ×400 magnification by randomly selecting 10 seminiferous tubules in a testis section from each animal and assessing the sections under a light microscope (Olympus BX51). Cells with red-stained nuclei were evaluated as positive. Both stained and non-stained germ cells were counted, and the ratio of stained cells to the total number of germ cells, multiplied by 100, gave the p-p38 MAPK index for each seminiferous tubule (calculated as %). The average p-p38 MAPK index in each animal was determined by taking the average of the indices of tubules [45,47].

By contrast, NF-κB immunoreactivity was semi-quantitatively evaluated with the H-score method. Assessments were made under a light microscope (Olympus BX-51) at ×400 magnification by randomly selecting five areas in transverse sections of the testis of each animal. The scores were generated by taking the percentage of cells with immunoreactivity in the sections (Pi) and the degree of staining (i). The degree of staining was assessed as 0 (no staining), 1 (weak staining), 2 (moderate staining), and 3 (strong staining). The average H-score for each section belonging to each animal was calculated with the following formula: H-score = $\Sigma i \times Pi$ [46]. All semiquantitative assessments by light microscopy were made by two independent observers and the averages were considered.

5. Statistical analysis

All statistical analyses were performed using the IBM SPSS ver. 20.0 (IBM Corp., Armonk, NY, USA; license no. 10240642). The results are expressed as mean ± standard deviation, and $p < 0.05$ were considered to indicate statistical significance. All data were assessed for normal distribution with the Kolmogorov-Smirnov test. The values showed a normal distribution, so one-way analysis of variance was carried out. Depending on the homogeneity of the groups, the Tukey or Tamhane multiple comparison test was used to determine the significance of differences between groups. The nonparametric Kruskal-Wallis test was used to determine the significance of changes in the body weight of the animals. The Bonferroni-corrected Mann-Whitney *U*-test was conducted to assess the significance of between-group differences.

Results

1. Body and testicular weight findings

The initial and final body weights of animals were measured at the beginning and end of the experiment, respectively. A significant reduction was observed in the body weight of MTX-treated animals compared to the control group ($p < 0.05$) (Table 1), whereas no change was observed in testes weight or in the testicular weight index ($p > 0.05$). Conversely, pretreatment with CMN before MTX treatment caused a significant increase in the body weight compared to the MTX group ($p < 0.05$) (Table 1).

2. Morphometric findings

The seminiferous tubule diameter and germinal epithelium height significantly decreased in the MTX group, while the interstitial space width significantly increased ($p < 0.001$) (Table 2), in comparison to the control group. The administration of CMN before MTX treatment significantly increased the seminiferous tubule diameter and the germinal epithelium height ($p < 0.05$) (Table 2), while the interstitial space width significantly decreased ($p < 0.001$) (Table 2).

3. Histological findings

Light microscopy examination of the testis tissue sections in the control group revealed active spermatogenesis and a regular and normal appearance of the seminiferous tubules. The incidence of detached, sloughed, or vacuolized seminiferous tubules were also very low. Eosinophilic Leydig cells appeared as clusters in the interstitial field located between the neighboring seminiferous tubules and had a normal histological structure (Figure 1A and B).

Examination of the testis tissue sections in the MTX group revealed degeneration and loss of germinal series cells, disorganization of the germ cell layers, and vacuolization in the seminiferous tubules. The number of damaged seminiferous tubules containing detached ($p < 0.001$), sloughed ($p < 0.001$), or vacuolized ($p < 0.001$) tubules was higher in the MTX group than in the control group, whereas the number of normal ($p < 0.001$) tubules was smaller. Sloughing of germinal cells that had not completed maturation in the lumen was also evident in the MTX group, and some seminiferous tubules showed irregularities and undulations of the basal membrane. No change was observed in Sertoli cells, but the interstitial space showed cell loss with edema (Figure 1C and D).

Spermatogenesis was markedly preserved in the MTX+CMN group. Moreover, the percentages of damaged seminiferous tubules with disorganization of the germ cell layers were markedly lower in this group. Irregularity and cell loss in the interstitial space width were also less common than in the MTX group, and edema was also reduced (Figure 1E and F). The scoring results for changes in the histological structure of the seminiferous tubules in all groups are summarized in Table 3.

4. Immunohistochemical findings

p-p38 MAPK immunopositive cells showed nuclear staining, mostly in primary spermatocytes, in the sections of seminiferous tubules. The control group showed low numbers of p-p38 MAPK immunopositive cells (Figure 2A). By contrast, sections of seminiferous tubules in the MTX group showed a significantly higher number of im-

Table 1. Comparison of changes in body weight, testis weight, and testis/body weight ratio ([weight of both testes/body weight] ×100) in rats in the control, methotrexate-treated, and methotrexate+curcumin-treated groups

Parameter	Control	Methotrexate	Methotrexate+curcumin
Change in body weight (g)	13.17 ± 5.00	–21.50 ± 6.16[a]	–9.33 ± 4.18[a),b)]
Weight of both testes (g)	2.52 ± 0.14	2.53 ± 0.12	2.52 ± 0.19
(Weight of both testes/body weight) × 100	0.97 ± 0.04	0.94 ± 0.06	0.94 ± 0.03

Values are presented as mean±standard deviation for six rats in each group.
[a]$p<0.05$, significant difference compared to the control group; [b]$p<0.05$, significant difference compared to the methotrexate group.

Table 2. Comparison of seminiferous tubule diameter, germinal epithelium height, and interstitial space width in testis tissues of rats in control, methotrexate-treated, and methotrexate+curcumin-treated groups

Parameter	Control	Methotrexate	Methotrexate+curcumin
Seminiferous tubule diameter (μm)	280.20 ± 6.91	250.65 ± 5.55[b]	267.67 ± 3.01[a),c)]
Germinal epithelium height (μm)	63.23 ± 0.84	48.80 ± 1.26[b]	58.27 ± 2.33[a),c)]
Interstitial space width (μm)	22.16 ± 1.80	39.53 ± 2.20[b]	30.22 ± 1.60[b),c)]

Values are presented as mean±standard deviation for six rats in each group.
[a]$p<0.05$, significant difference compared to the control group; [b]$p<0.001$, significant difference compared to the control group; [c]$p<0.001$, significant difference compared to the methotrexate group.

https://doi.org/10.5653/cerm.2020.04105

munopositive cells ($p < 0.001$) (Figure 2C), whereas the tubules in the MTX+CMN group showed a significant suppression of this increase ($p < 0.001$) (Figure 2E). No staining was observed in the negative control group (Figure 2G).

The testicular seminiferous tubules of the control group showed cytoplasmic NF-κB immunoreactivity with weak intensity in primary spermatocytes and very weak intensity in spermatids, with no immunoreactivity apparent in spermatogonia and Sertoli cells. Similar-

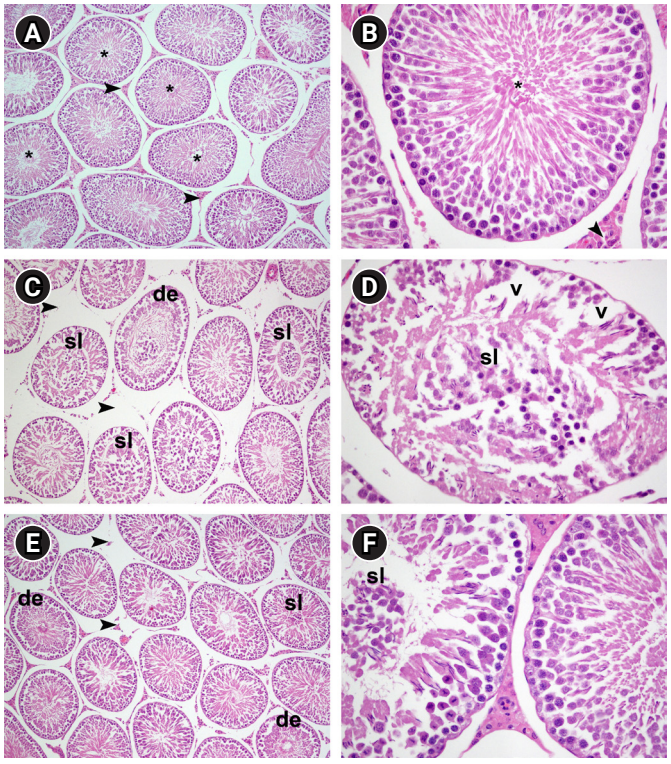

Figure 1. Light microscopy of testicular tissue of rats in control (A, B), methotrexate-treated (C, D), and methotrexate+curcumin-treated (E, F) groups. (A, B) Regular seminiferous tubules (asterisks) and normal interstitial space (arrowheads). (C, D) Irregular, detached (de), sloughed (sl), and vacuolized (v) seminiferous tubules and interstitial edema (arrowheads). (E, F) Highly regular and restored testicular tissue showing only a few histologically damaged detached (de) or sloughed (sl) seminiferous tubules and mild interstitial edema (arrowheads). H&E (A, C, E: ×100; B, D, F : ×400).

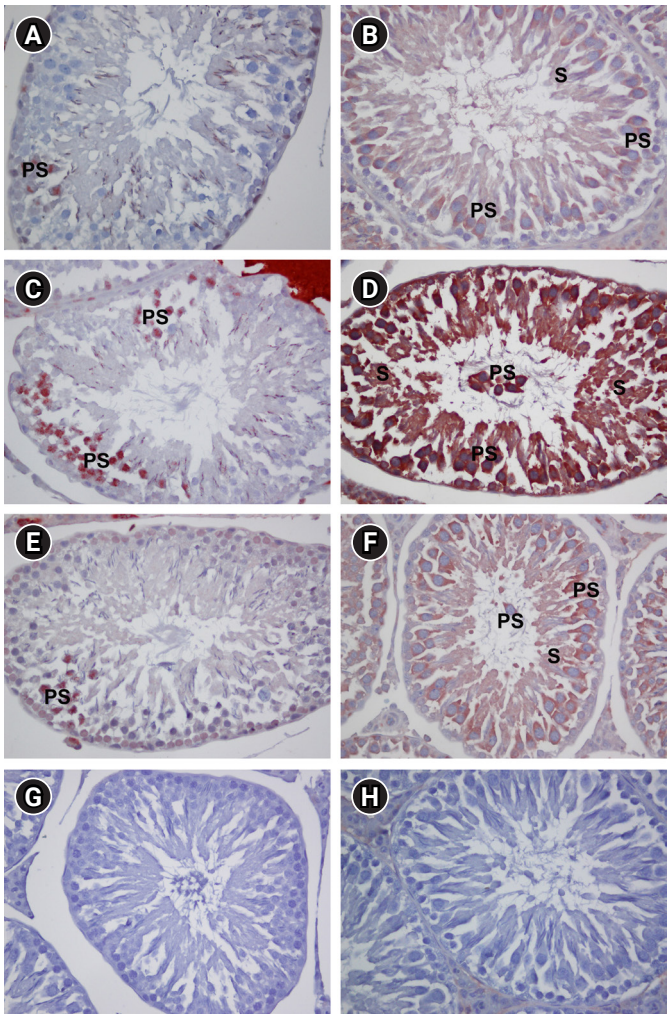

Figure 2. Phospho-p38 (p-p38) mitogen-activated protein kinase (MAPK) immunopositive cells and nuclear factor-kappa B (NF-κB) immunoreactivity in testicular tissues of control (A, B), methotrexate-treated (C, D), and methotrexate+curcumin-treated (E, F) groups. Negative controls for p-p38 MAPK and NF-κB, respectively (G, H). PS, primary spermatocyte; S, spermatid. H&E (×400).

Table 3. Comparison of the histologic structure of seminiferous tubules in testis tissues of rats in the control, methotrexate-treated, and methotrexate+curcumin-treated groups

Percentage of seminiferous tubules	Control	Methotrexate	Methotrexate+curcumin
Normal	95.01 ± 1.04	31.08 ± 6.17[a)]	67.14 ± 4.83[a),c)]
Detached	3.03 ± 0.87	27.84 ± 4.13[a)]	14.26 ± 1.82[a),b)]
Sloughed	0.80 ± 0.32	25.28 ± 6.24[a)]	11.17 ± 1.89[a),b)]
Vacuolized	1.16 ± 0.51	22.23 ± 3.66[a)]	10.18 ± 1.93[a),c)]

Values are presented as mean ± standard deviation for six rats in each group.
[a)]$p<0.001$, significant difference compared to the control group; [b)]$p<0.05$, significant difference compared to the methotrexate group; [c)]$p<0.001$, significant difference compared to the methotrexate group.

ly, no immunoreactivity was observed in Leydig cells in the interstitial space (Figure 2B). Sections of the seminiferous tubules in the MTX group showed strong immunoreactivity in primary spermatocytes and moderately strong reactivity in spermatids, but only weak to moderate reactivity in spermatogonia. Immunoreactivity was weak in Sertoli cells and moderately weak in Leydig cells (Figure 2D). The NF-κB immunoreactivity of the MTX group was statistically significantly higher than that of the control group ($p < 0.001$). An examination of seminiferous tubule sections from the MTX+CMN group revealed significantly lower immunoreactivity for NF-κB than in the MTX group ($p < 0.001$). Staining was still moderate in spermatocytes and was mostly weak in spermatids and spermatogonia. Weak staining was also seen in Leydig cells. No staining was observed in Sertoli cells (Figure 2F). No staining was encountered in the negative control group (Figure 2H).

For all groups, the p-p38 MAPK index was determined by evaluating the p-p38 MAPK positive cell number (%) and NF-κB immunoreactivity was determined from the H-score in seminiferous tubules. These values are summarized in Table 4.

Discussion

MTX, an anticancer drug commonly used in chemotherapy, is a folic acid antagonist that belongs to the group of drugs known as antimetabolites [25,48,49]. Folic acid is an important dietary factor that is converted to tetrahydrofolate, an important carbon source for the synthesis of DNA (thymidylate and purines) and RNA (purines) precursors by enzymatic reduction [50]. MTX inhibits dihydrofolate reductase (DHFR). It causes the depletion of dihydrofolate and inhibits DNA synthesis indirectly by affecting thymidine synthesis [51]. Inhibition of DHFR leads to partial depletion of tetrahydrofolate cofactors requisite for related thymidylate and purine synthesis [50].

Previous studies have shown that MTX affects spermatogenesis by causing damage to the male reproductive system [21,22,25,44,52]. Some studies have used various chemical agents to protect against the testicular damage caused by MTX [21,22,24,25,27,53]. Therefore, the present study aimed to analyze the protective effect of CMN against MTX-induced testicular damage by histological and immunohistochemical analyses of the p-p38 MAPK and NF-κB signaling pathways.

A comparison of the body weights of the animals at the beginning and the end of our study revealed a significant weight loss in the MTX group compared to the control group, but this weight loss was ameliorated in the MTX+CMN group. This observation of weight loss in the MTX group is supported by several studies [54-56]. However, a study conducted by Padmanabhan et al. [57] reported that two groups with different experimental periods (5 and 10 weeks) given 4 different weekly doses of MTX (5, 10, 20, and 40 mg/kg) did not show significant weight loss after a short treatment duration, but showed a significant reduction with a longer duration, in agreement with our study. Another study carried out in mice by Padmanabhan et al. [53] also showed a certain reduction in body weight in a group given MTX for 10 weeks at a dose of 20 mg/kg once in a week, but the decrease was not considered statistically significant.

When testicular weight (both testes) was examined, no significant difference was observed between groups. Similarly, the total TWI did not significantly differ between groups. Many other studies have also found no significant differences, in agreement with our results [23,53,54,56,57]. The lack of any difference in testicular weight could be explained by compensation for the reduction in the seminiferous tubule diameter caused by MTX through the possible formation of edema in the interstitial space in response to MTX. An evaluation of the testicular weight index (the ratio of total testis weight/total body weight) revealed no statistically significant differences among all three groups in our study. Padmanabhan et al. [53,57] also reported that MTX administration did not affect the testicular weight index, whereas El-Sheikh et al. [55] demonstrated a significant reduction in this ratio at the end of the ninth day.

In our study, the MTX group showed a significantly lower diameter of the seminiferous tubules than the control group. Other studies that used a single dose of 20 mg/kg of MTX, as in our study, also showed decreases in the diameters of the seminiferous tubules [22,24,25]. Furthermore, other studies that used low doses daily and weekly also reported decreases in the diameter of the seminiferous tubules and damage to the germinal epithelium [26,56,58].

The MTX-treated tissues in the present study also showed a de-

Table 4. Comparison of the p-p38 MAPK index and NF-κB immunoreactivity in testis tissues of rats in the control, methotrexate-treated, and methotrexate+curcumin-treated groups

Parameter	Control	Methotrexate	Methotrexate+curcumin
p-p38 MAPK index (%)	3.24 ± 1.11	12.55 ± 2.40[b]	7.39 ± 1.35[a),c)]
NF-κB immunoreactivity	86.67 ± 13.66	237.50 ± 18.37[b]	150.00 ± 17.89[b),c)]

Values are presented as mean±standard deviation for six rats in each group.
p-p38, phospho-p38; MAPK, mitogen-activated protein kinase; NF-κB, nuclear factor-kappa B.
[a] $p<0.05$, significant difference compared to the control group; [b] $p<0.001$, significant difference compared to the control group; [c] $p<0.001$, significant difference compared to the methotrexate group.

https://doi.org/10.5653/cerm.2020.04105

crease in germinal epithelium height. This reduction, as well as the decrease in tubule diameter, could be the result of the decreased diameter of the cells forming the germinal epithelium and/or the sloughing of immature germinal cells into the tubule lumen due to DNA damage caused by MTX. In parallel to our study, some studies have reported decreases in the height of the germinal epithelium as a result of MTX injection [26,52,56]. Other studies have also shown that the measured diameters of spermatocytes and spermatids found within the tubules were significantly lower than those in the control group [58,59]. No changes were found in a study that measured the diameters of Sertoli cells [58].

In the present study, the interstitial space was significantly wider in the MTX group than in the control group. A similar study carried out by Oufi and Al-Shawi. [25] also reported an increase in the width of the interstitial space in an MTX-treated group. Another study also found a significant increase in the width of the interstitial space in histological sections from the testes of rats given MTX [58]. Conversely, Nouri et al. [56] used two different experimental periods and found no significant change in a short period after MTX treatment, but observed a significant increase in the width of the interstitial space at the end of a long experimental period.

The changes in the histological structure of the seminiferous tubules examined in this study were classified as normal, detached, sloughed, or vacuolized. The MTX group showed significantly fewer normal seminiferous tubules than the control group, while significantly more detached, sloughed, or vacuolized seminiferous tubules were observed. The studies carried out by Padmanabhan et al. [53,57] support these results. In our study, histological damage in the testes caused by MTX was observed in the seminiferous tubules, as shown by disorganization of germ cell layers and sloughing of germinal cells that had not completed maturation into the tubule lumen. Degeneration and loss of germinal series cells, disorganization of germ cell layers, and vacuolization in the seminiferous tubules were also observed. Some seminiferous tubules also showed irregularities and undulations of the basal membrane. Our observations of histological damages are consistent with earlier reports [8,22]. No change was observed in Sertoli cells, but the interstitial space showed cell loss and edema.

In this study, no significant difference was observed in the testicular weight index among the groups. The diameter of the seminiferous tubules and the height of the epithelium were significantly larger and the width of the interstitial space was significantly smaller in the MTX+CMN group than in the MTX group. The structure of the seminiferous tubules in the MTX +CMN group showed fewer damaged tubules containing detached, sloughed, or vacuolized tubules than in the MTX group. The tubules also had a fairly normal structure compared to those of the MTX group.

In our study, the assessment of p-p38 MAPK immunopositive staining in the MTX group revealed staining in the primary spermatocytes in most seminiferous tubules. In the MTX group, particularly strong NF-κB immunoreactivity was observed in primary spermatocytes, while staining was moderately strong in spermatids and weak to moderate in spermatogonia. The Sertoli cells showed weak immunoreactivity in the MTX group, but CMN administration significantly decreased the numbers of p-p38 MAPK positive cells and NF-κB immunoreactivity. An MTX-induced increase in the NF-κB activation in testes has previously been reported [55], as has an increase in p38 MAPK protein levels in bronchial cell culture in response to MTX [14]. Increases in NF-κB and p38 MAPK signaling have also been reported in testicular tissues damaged by other agents [43].

In our study, MTX administration was found to damage the seminiferous tubules, as shown by abnormal histological and immunohistochemical findings. In connection with our study, a previous study using of MTX showed upregulation of NF-κB protein expression after testis injuries, while administration of melatonin (an anti-inflammatory and antioxidant agent) downregulated NF-κB protein expression [60]. In another study, male obesity disrupted the balance between oxidation and antioxidation in the testicular tissue, upregulated NF-κB, increased inflammation, and disrupted sperm quality, thereby negatively affecting male reproductive function [61]. If increased NF-κB signaling initiates the inflammatory process, lower sperm production and a decrease in the fertilization rate will be observed due to MTX-induced upregulation of NF-κB, as in our study.

Previous studies showed that MAPKs were linked with disruption of sperm production [62,63]. The mitochondrial apoptosis pathway induced by activated p38 MAPK resulted in a breakdown in spermatogenesis, defective sperm formation, and consequently infertility [62,64]. In our study, the number of p-p38 MAPK immunopositive cells increased in animals with MTX-induced testicular injuries. According to previous studies [62-64], increased p-p38 MAPK expression after MTX-induced testis injuries may cause a decrease in the number of sperm and the fertilization rate.

p38 MAPK is a kinase that can be activated by a variety of cellular stresses, including oxidative stress. This kinase is mainly related to inflammation and apoptosis. By contrast, NF-κB is a dimeric transcription factor composed of different members that can activate a diverse range of genes related to stress responses, inflammation, and apoptosis [65]. Several studies have shown that CMN decreases both p-p38 MAPK and NF-κB activation [43,66-68]. The results presented here also demonstrated that CMN could significantly suppress the MTX-induced increase in p-p38 MAPK and NF-κB expression in rat testis tissue.

CMN is known to possess antioxidant, anti-inflammatory, and antitumoral properties [28,30,32,34]. Several studies have shown that

CMN can reduce the side effects of MTX in non-testicular tissues [28,32,69]. CMN has also demonstrated effectiveness against testicular damage induced by other agents, as reported by several investigators [43,70].

Taken together, our results and previous findings indicate that CMN may reduce MTX-induced testicular damage by suppressing the p38 MAPK and NF-κB signaling pathways. Therefore, CMN may represent a promising candidate for the treatment of male infertility caused by MTX.

Conflict of interest

No potential conflict of interest relevant to this article was reported.

ORCID

Leyla Kilinc https://orcid.org/0000-0002-0946-2565
Yesim Hulya Uz https://orcid.org/0000-0002-0381-4590

Author contributions

Conceptualization: YHU. Data curation: LK. Formal analysis: all authors. Funding acquisition: LK. Methodology: all authors. Project administration: YHU. Visualization: all authors. Writing–original draft: LK. Writing–review & editing: all authors.

References

1. Cole PD, Zebala JA, Alcaraz MJ, Smith AK, Tan J, Kamen BA. Pharmacodynamic properties of methotrexate and Aminotrexate during weekly therapy. Cancer Chemother Pharmacol 2006;57:826–34.
2. Hashkes PJ, Becker ML, Cabral DA, Laxer RM, Paller AS, Rabinovich CE, et al. Methotrexate: new uses for an old drug. J Pediatr 2014;164:231–6.
3. Weber-Schoendorfer C, Hoeltzenbein M, Wacker E, Meister R, Schaefer C. No evidence for an increased risk of adverse pregnancy outcome after paternal low-dose methotrexate: an observational cohort study. Rheumatology (Oxford) 2014;53:757–63.
4. Sener G, Eksioglu-Demiralp E, Cetiner M, Ercan F, Sirvanci S, Gedik N, et al. L-Carnitine ameliorates methotrexate-induced oxidative organ injury and inhibits leukocyte death. Cell Biol Toxicol 2006;22:47–60.
5. Semet M, Paci M, Saias-Magnan J, Metzler-Guillemain C, Boissier R, Lejeune H, et al. The impact of drugs on male fertility: a review. Andrology 2017;5:640–63.
6. Aslankoc R, Ozmen O, Ellidag HY. Ameliorating effects of agomelatine on testicular and epididymal damage induced by methotrexate in rats. J Biochem Mol Toxicol 2020;34:e22445.
7. Daggulli M, Dede O, Utangac MM, Bodakci MN, Hatipoglu NK, Penbegul N, et al. Protective effects of carvacrol against methotrexate-induced testicular toxicity in rats. Int J Clin Exp Med 2014;7:5511–6.
8. Oktar S, Gokce A, Aydin M, Davarci M, Meydan S, Ozturk OH, et al. Beneficial effect of erdosteine on methotrexate-induced testicular toxicity in mice. Toxicol Ind Health 2010;26:433–8.
9. Morris LF, Harrod MJ, Menter MA, Silverman AK. Methotrexate and reproduction in men: case report and recommendations. J Am Acad Dermatol 1993;29(5 Pt 2):913–6.
10. Morrison DK. MAP kinase pathways. Cold Spring Harb Perspect Biol 2012;4:a011254.
11. Grab J, Rybniker J. The expanding role of p38 mitogen-activated protein kinase in programmed host cell death. Microbiol Insights 2019;12:1178636119864594.
12. Segreto HR, Oshima CT, Franco MF, Silva MR, Egami MI, Teixeira VP, et al. Phosphorylation and cytoplasmic localization of MAPK p38 during apoptosis signaling in bone marrow granulocytes of mice irradiated in vivo and the role of amifostine in reducing these effects. Acta Histochem 2011;113:300–7.
13. Shen L, Tang X, Wei Y, Long C, Tan B, Wu S, et al. Vitamin E and vitamin C attenuate Di-(2-ethylhexyl) phthalate-induced blood-testis barrier disruption by p38 MAPK in immature SD rats. Reprod Toxicol 2018;81:17–27.
14. Kim YJ, Song M, Ryu JC. Inflammation in methotrexate-induced pulmonary toxicity occurs via the p38 MAPK pathway. Toxicology 2009;256:183–90.
15. Cho HW, Park SK, Heo KW, Hur DY. Methotrexate induces apoptosis in nasal polyps via caspase cascades and both mitochondria-mediated and p38 mitogen-activated protein kinases/Jun N-terminal kinase pathways. Am J Rhinol Allergy 2013;27:e26–31.
16. Beutheu Youmba S, Belmonte L, Galas L, Boukhettala N, Bole-Feysot C, Dechelotte P, et al. Methotrexate modulates tight junctions through NF-κB, MEK, and JNK pathways. J Pediatr Gastroenterol Nutr 2012;54:463–70.
17. King TJ, Georgiou KR, Cool JC, Scherer MA, Ang ES, Foster BK, et al. Methotrexate chemotherapy promotes osteoclast formation in the long bone of rats via increased pro-inflammatory cytokines and enhanced NF-κB activation. Am J Pathol 2012;181:121–9.
18. Mukherjee S, Ghosh S, Choudhury S, Adhikary A, Manna K, Dey S, et al. Pomegranate reverses methotrexate-induced oxidative stress and apoptosis in hepatocytes by modulating Nrf2-NF-κB pathways. J Nutr Biochem 2013;24:2040–50.
19. van't Land B, Blijlevens NM, Marteijn J, Timal S, Donnelly JP, de

https://doi.org/10.5653/cerm.2020.04105

Witte TJ, et al. Role of curcumin and the inhibition of NF-kappaB in the onset of chemotherapy-induced mucosal barrier injury. Leukemia 2004;18:276–84.

20. Karin M, Cao Y, Greten FR, Li ZW. NF-kappaB in cancer: from innocent bystander to major culprit. Nat Rev Cancer 2002;2:301–10.
21. Belhan S, Comakli S, Kucukler S, Gulyuz F, Yildirim S, Yener Z. Effect of chrysin on methotrexate-induced testicular damage in rats. Andrologia 2019;51:e13145.
22. Gokce A, Oktar S, Koc A, Yonden Z. Protective effects of thymoquinone against methotrexate-induced testicular injury. Hum Exp Toxicol 2011;30:897–903.
23. Koc F, Erisgin Z, Tekelioglu Y, Takir S. The effect of beta glucan on MTX induced testicular damage in rats. Biotech Histochem 2018;93:70–5.
24. Maremanda KP, Jena GB. Methotrexate-induced germ cell toxicity and the important role of zinc and SOD1: Investigation of molecular mechanisms. Biochem Biophys Res Commun 2017;483:596–601.
25. Oufi HG, Al-Shawi NN. The effects of different doses of silibinin in combination with methotrexate on testicular tissue of mice. Eur J Pharmacol 2014;730:36–40.
26. Pinar N, Cakirca G, Ozgur T, Kaplan M. The protective effects of alpha lipoic acid on methotrexate induced testis injury in rats. Biomed Pharmacother 2018;97:1486–92.
27. Yulug E, Turedi S, Alver A, Turedi S, Kahraman C. Effects of resveratrol on methotrexate-induced testicular damage in rats. ScientificWorldJournal 2013;2013:489659.
28. Hemeida RA, Mohafez OM. Curcumin attenuates methotraxate-induced hepatic oxidative damage in rats. J Egypt Natl Canc Inst 2008;20:141–8.
29. Jantan I, Bukhari SN, Lajis NH, Abas F, Wai LK, Jasamai M. Effects of diarylpentanoid analogues of curcumin on chemiluminescence and chemotactic activities of phagocytes. J Pharm Pharmacol 2012;64:404–12.
30. Liu F, Gao S, Yang Y, Zhao X, Fan Y, Ma W, et al. Antitumor activity of curcumin by modulation of apoptosis and autophagy in human lung cancer A549 cells through inhibiting PI3K/Akt/mTOR pathway. Oncol Rep 2018;39:1523–31.
31. Sun L, Liu Z, Wang L, Cun D, Tong HH, Yan R, et al. Enhanced topical penetration, system exposure and anti-psoriasis activity of two particle-sized, curcumin-loaded PLGA nanoparticles in hydrogel. J Control Release 2017;254:44–54.
32. Wang Q, Ye C, Sun S, Li R, Shi X, Wang S, et al. Curcumin attenuates collagen-induced rat arthritis via anti-inflammatory and apoptotic effects. Int Immunopharmacol 2019;72:292–300.
33. Yang R, Wang J, Zhou Z, Qi S, Ruan S, Lin Z et al. Curcumin promotes burn wound healing in mice by upregulating caveolin-1 in epidermal stem cells. Phytother Res 2019;33:422–30.
34. Moshari S, Nejati V, Najafi G, Razi M. Nanomicelle curcumin-induced DNA fragmentation in testicular tissue: correlation between mitochondria dependent apoptosis and failed PCNA-related hemostasis. Acta Histochem 2017;119:372–81.
35. Moreira-Pinto B, Costa L, Fonseca BM, Rebelo I. Dissimilar effects of curcumin on human granulosa cells: beyond its anti-oxidative role. Reprod Toxicol 2020;95:51–8.
36. Itokawa H, Shi Q, Akiyama T, Morris-Natschke SL, Lee KH. Recent advances in the investigation of curcuminoids. Chin Med 2008;3:11.
37. Nagpal M, Sood S. Role of curcumin in systemic and oral health: an overview. J Nat Sci Biol Med 2013;4:3–7.
38. Choudhary D, Chandra D, Kale RK. Modulation of radioresponse of glyoxalase system by curcumin. J Ethnopharmacol 1999;64:1–7.
39. Mahmood K, Zia KM, Zuber M, Salman M, Anjum MN. Recent developments in curcumin and curcumin based polymeric materials for biomedical applications: a review. Int J Biol Macromol 2015;81:877–90.
40. Ulubay M, Alkan I, Yurt KK, Kaplan S. The protective effect of curcumin on the diabetic rat kidney: a stereological, electron microscopic and immunohistochemical study. Acta Histochem 2020;122:151486.
41. Aydin MS, Caliskan A, Kocarslan A, Kocarslan S, Yildiz A, Gunay S, et al. Intraperitoneal curcumin decreased lung, renal and heart injury in abdominal aorta ischemia/reperfusion model in rat. Int J Surg 2014;12:601–5.
42. Song WB, Wang YY, Meng FS, Zhang QH, Zeng JY, Xiao LP, et al. Curcumin protects intestinal mucosal barrier function of rat enteritis via activation of MKP-1 and attenuation of p38 and NF-κB activation. PLoS One 2010;5:e12969.
43. Ilbey YO, Ozbek E, Cekmen M, Simsek A, Otunctemur A, Somay A. Protective effect of curcumin in cisplatin-induced oxidative injury in rat testis: mitogen-activated protein kinase and nuclear factor-kappa B signaling pathways. Hum Reprod 2009;24:1717–25.
44. Vardi N, Parlakpinar H, Ates B, Cetin A, Otlu A. Antiapoptotic and antioxidant effects of beta-carotene against methotrexate-induced testicular injury. Fertil Steril 2009;92:2028–33.
45. Orazizadeh M, Khorsandi L, Absalan F, Hashemitabar M, Daneshi E. Effect of beta-carotene on titanium oxide nanoparticles-induced testicular toxicity in mice. J Assist Reprod Genet 2014;31:561–8.
46. Uz YH, Murk W, Bozkurt I, Kizilay G, Arici A, Kayisli UA. Increased c-Jun N-terminal kinase activation in human endometriotic endothelial cells. Histochem Cell Biol 2011;135:83–91.
47. Altay B, Cetinkalp S, Doganavsargil B, Hekimgil M, Semerci B. Streptozotocin-induced diabetic effects on spermatogenesis with proliferative cell nuclear antigen immunostaining of adult rat tes-

tis. Fertil Steril 2003;80 Suppl 2:828–31.
48. Caglar Y, Ozgur H, Matur I, Yenilmez ED, Tuli A, Gonlusen G, et al. Ultrastructural evaluation of the effect of N-acetylcysteine on methotrexate nephrotoxicity in rats. Histol Histopathol 2013;28:865–74.
49. Chabner BA, Allegra CJ, Curt GA, Clendeninn NJ, Baram J, Koizumi S, et al. Polyglutamation of methotrexate. Is methotrexate a prodrug? J Clin Invest 1985;76:907–12.
50. Chabner BA, Amrein PC, Druker BJ, Michaelson MD, Mitsiades CS, Goss PE, et al. Chemotherapy of neoplastic diseases. Chemotherapy of neoplastic diseases. In: Brunton LL, Lazo JS, Parker KL, editors. Goodman and Gilman's the pharmacological basis of therapeutics. New York: McGraw-Hill; 2006. p. 1335-6.
51. Babiak RM, Campello AP, Carnieri EG, Oliveira MB. Methotrexate: pentose cycle and oxidative stress. Cell Biochem Funct 1998; 16:283–93.
52. Sukhotnik I, Nativ O, Roitburt A, Bejar D, Coran AG, Mogilner JG, et al. Methotrexate induces germ cell apoptosis and impairs spermatogenesis in a rat. Pediatr Surg Int 2013;29:179–84.
53. Padmanabhan S, Tripathi DN, Vikram A, Ramarao P, Jena GB. Methotrexate-induced cytotoxicity and genotoxicity in germ cells of mice: intervention of folic and folinic acid. Mutat Res 2009;673: 43–52.
54. Armagan A, Uzar E, Uz E, Yilmaz HR, Kutluhan S, Koyuncuoglu HR, et al. Caffeic acid phenethyl ester modulates methotrexate-induced oxidative stress in testes of rat. Hum Exp Toxicol 2008; 27:547–52.
55. El-Sheikh AA, Morsy MA, Al-Taher AY. Multi-drug resistance protein (Mrp) 3 may be involved in resveratrol protection against methotrexate-induced testicular damage. Life Sci 2014;119:40–6.
56. Nouri HS, Azarmi Y, Movahedin M. Effect of growth hormone on testicular dysfunction induced by methotrexate in rats. Andrologia 2009;41:105–10.
57. Padmanabhan S, Tripathi DN, Vikram A, Ramarao P, Jena GB. Cytotoxic and genotoxic effects of methotrexate in germ cells of male Swiss mice. Mutat Res 2008;655:59–67.
58. Saxena AK, Dhungel S, Bhattacharya S, Jha CB, Srivastava AK. Effect of chronic low dose of methotrexate on cellular proliferation during spermatogenesis in rats. Arch Androl 2004;50:33–5.
59. Shrestha S, Dhungel S, Saxena AK, Bhattacharya S, Maskey D. Effect of methotrexate (MTX) administration on spermatogenesis: an experimental on animal model. Nepal Med Coll J 2007; 9:230–3.
60. Wang Y, Zhao TT, Zhao HY, Wang H. Melatonin protects methotrexate-induced testicular injury in rats. Eur Rev Med Pharmacol Sci 2018;22:7517–25.
61. Yi X, Tang D, Cao S, Li T, Gao H, Ma T, et al. Effect of different exercise loads on testicular oxidative stress and reproductive function in obese male mice. Oxid Med Cell Longev 2020;2020:3071658.
62. Taha SH, Zaghloul HS, Ali AA, Rashed LA, Sabry RM, Gaballah IF. Molecular and hormonal changes caused by long-term use of high dose pregabalin on testicular tissue: the role of p38 MAPK, oxidative stress and apoptosis. Mol Biol Rep 2020;47:8523–33.
63. Li MW, Mruk DD, Cheng CY. Mitogen-activated protein kinases in male reproductive function. Trends Mol Med 2009;15:159–68.
64. Xiong X, Zhang L, Fan M, Han L, Wu Q, Liu S, et al. β-Endorphin induction by psychological stress promotes Leydig cell apoptosis through p38 MAPK pathway in male rats. Cells 2019;8:1265.
65. Wang T, Zhang X, Li JJ. The role of NF-kappaB in the regulation of cell stress responses. Int Immunopharmacol 2002;2:1509–20.
66. Camacho-Barquero L, Villegas I, Sanchez-Calvo JM, Talero E, Sanchez-Fidalgo S, Motilva V, et al. Curcumin, a Curcuma longa constituent, acts on MAPK p38 pathway modulating COX-2 and iNOS expression in chronic experimental colitis. Int Immunopharmacol 2007;7:333–42.
67. Chauhan PS, Singh DK, Dash D, Singh R. Intranasal curcumin regulates chronic sthma in mice by modulating NF-κB activation and MAPK signaling. Phytomedicine 2018;51:29–38.
68. Geng S, Wang S, Zhu W, Xie C, Li X, Wu J, et al. Curcumin suppresses JNK pathway to attenuate BPA-induced insulin resistance in LO2 cells. Biomed Pharmacother 2018;97:1538–43.
69. Morsy MA, Ibrahim SA, Amin EF, Kamel MY, Rifaai RA, Hassan MK. Curcumin ameliorates methotrexate-induced nephrotoxicity in rats. Adv Pharmacol Sci 2013;2013:387071.
70. Glombik K, Basta-Kaim A, Sikora-Polaczek M, Kubera M, Starowicz G, Styrna J. Curcumin influences semen quality parameters and reverses the di(2-ethylhexyl)phthalate (DEHP)-induced testicular damage in mice. Pharmacol Rep 2014;66:782–7.

https://doi.org/10.5653/cerm.2020.04105